Respiratory Phase Affects the Conspicuity of CSF–Venous Fistulas in Spontaneous Intracranial Hypotension

T.J. Amrhein, L. Gray, M.D. Malinzak, and P.G. Kranz

ABSTRACT

SUMMARY: Spinal CSF–venous fistulas are a cause of spontaneous intracranial hypotension that can be difficult to detect on imaging. We describe how the respiratory phase affects the visibility of CSF–venous fistulas during myelography.

ABBREVIATIONS: CTM = CT myelography; CVF = CSF–venous fistula; SIH = spontaneous intracranial hypotension

Spontaneous intracranial hypotension (SIH) is a debilitating condition caused by spinal CSF leaks and CSF–venous fistulas (CVFs).[1] The localization of these spinal causes of SIH is critical for successful treatment.[2,3] CVFs are particularly difficult to identify on traditional myelographic imaging.[1,4] Technical modifications to the myelography technique such as decubitus imaging during dynamic myelography, digital subtraction myelography, and CT myelography (CTM) have been shown to improve the conspicuity of CVFs, which are often subtle.[5] However, additional methods for maximizing CVF identification remain desirable. We have observed that the ability to visualize CVFs varies with different phases of respiration, suggesting that attention to the respiratory phase of imaging may improve their detection in some patients.

MATERIALS AND METHODS

Subjects

This was a retrospective case series of 5 patients with SIH treated at a single major referral institution from January 2018 to February 2020. All patients met the International Classification of Headache Disorders-3 criteria for SIH and had preprocedural contrast-enhanced brain MR imaging that was positive for SIH.[6,7] Patients were included when the conspicuity of a spinal CVF was affected by the respiratory phase during image acquisition. In all cases, an initial prone CTM demonstrated findings suggestive of a spinal CVF, necessitating further myelography in the ipsilateral decubitus position. This study was Health Insurance Portability and Accountability Act–compliant and was approved by the institutional internal review board with a waiver of informed consent.

Myelogram Technique

Decubitus myelography was performed in all cases due to subtle findings suggestive of a spinal CVF on a prior prone CTM. Decubitus myelograms were obtained as previously described using 10 mL of iopamidol containing 300 mg/mL of iodine (Isovue-M 300; Bracco).[5] Dynamic myelograms were all obtained on the same C-arm fluoroscopy unit equipped with a tilting table (MultiDiagnost Eleva; Philips Healthcare). Digital subtraction was not used. CTMs were all performed on a single 64–detector row CT scanner (Discovery 750HD; GE Healthcare) with the following parameters: helical scan mode, rotation time = 0.8 seconds, pitch = 0.969, tube voltage = 120 kV (peak), automated exposure control, tube current = 300–800 mA, noise index = 19.5, section thickness = 2.5 mm, interval = 2.5 mm, reconstruction thickness = 0.625 mm. Imaging was focused over the nerve root associated with the suspected CVF to limit the radiation dose. In 4 of the 5 patients, both a dynamic myelogram and a CTM in the decubitus position were obtained. In the other patient, only a decubitus CTM was performed. Images were obtained during breath-hold for all cases at various phases of the respiratory cycle (eg, neutral, full inspiration, and full expiration).

RESULTS

Subjects

The mean patient age was 60 years (range, 44–68 years), and 40% were women. All patients in this series coincidentally had undergone 2 CTMs before images were acquired with attention to the phase of the respiratory cycle. In all patients, 1 of the 2 prior CTMs had negative findings, and the other demonstrated a subtle finding suspicious for a CVF, which formed the basis for the

Received March 28, 2020; accepted after revision May 5.

From the Department of Radiology, Duke University Medical Center, Durham, North Carolina.

Please address correspondence to Timothy J. Amrhein, MD, Department of Radiology, Box 3808, Duke University Medical Center, Durham, NC 27710; e-mail: timothy.amrhein@duke.edu; @TimAmrheinMD

http://dx.doi.org/10.3174/ajnr.A6663

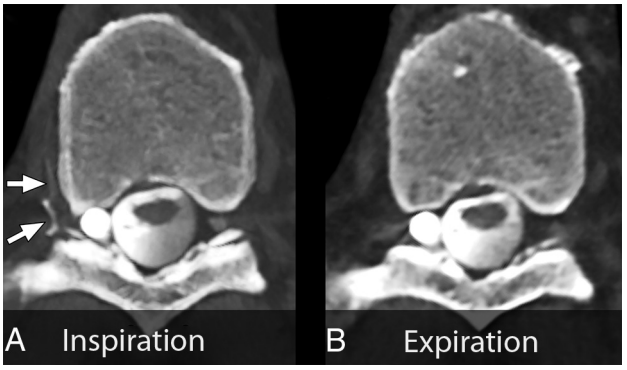

FIG 1. Maximum-intensity-projection CT myelograms of a right T9 nerve root sleeve CSF–venous fistula. *A*, Image acquisition during inspiration. Marked increased conspicuity of the CSF–venous fistula and hyperdense paraspinal vein (*arrows*). *B*, Image during expiration. The CSF–venous fistula is no longer visible.

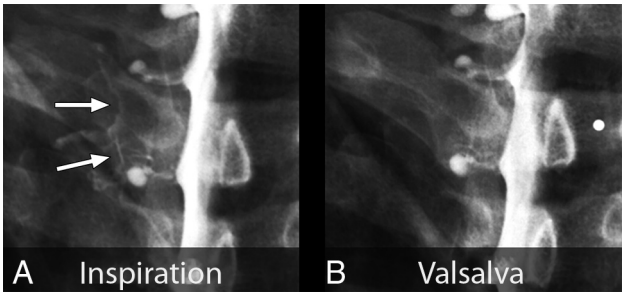

FIG 2. Spot-magnified radiographs of a left T2 nerve root sleeve CSF–venous fistula during an ipsilateral decubitus dynamic myelogram. *A*, Image acquired during inspiration demonstrates well the contrast-opacified CSF–venous fistula (*arrows*). *B*, Image during a Valsalva maneuver results in considerably reduced visualization of the CSF–venous fistula.

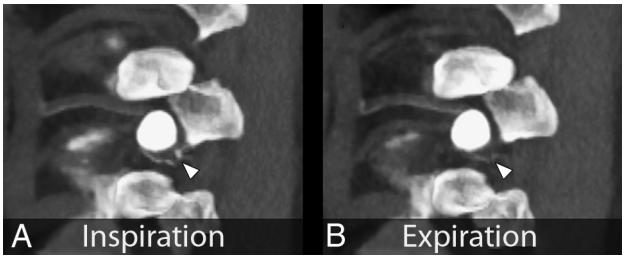

FIG 3. Parasagittal maximum-intensity-projection CT myelograms through the neuroforamen of a left T10 CSF–venous fistula. *A*, Image acquired during inspiration clearly captures contrast within the CSF–venous fistula (*arrowhead*). *B*, Image acquired during expiration. Note the markedly reduced conspicuity of the CSF–venous fistula (*arrowhead*).

decision to acquire the images depicted in this report. CVFs all originated from nerve root sleeves, consistent with previous reports, and were identified on the right at T9 and on the left at C8, T2, T8, and T10.[8]

Myelogram Findings

Images were acquired with breath-hold during various phases of the respiratory cycle, with the patient in the lateral decubitus

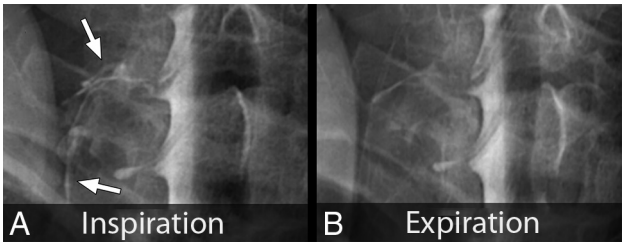

FIG 4. Spot-magnified radiographs of a left C8 CSF–venous fistula during an ipsilateral decubitus dynamic myelogram. *A*, Image acquired during inspiration demonstrates increased visibility and extent of the CSF–venous fistula (*arrows*). *B*, Image acquired during expiration leads to reduced visibility and extent of the CSF–venous fistula.

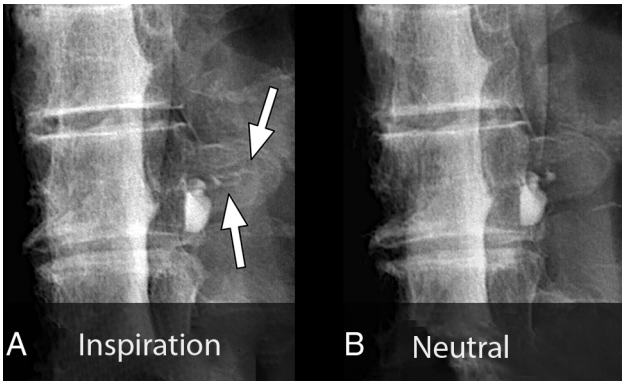

FIG 5. Spot-magnified radiographs of a left T8 CSF–venous fistula during an ipsilateral decubitus dynamic myelogram. *A*, Image acquired during inspiration demonstrates contrast opacification of the CSF–venous fistula extending out over the transverse process (*arrows*). *B*, Image acquired during quiet breath-hold during the mid-respiratory cycle. The CSF–venous fistula is no longer visible over the transverse process.

position. Inspiratory imaging was compared with additional phases of respiration including expiration ($n = 3$), neutral breath hold ($n = 1$), and Valsalva ($n = 1$). In all 5 patients, the CVF was more conspicuous during the inspiratory phase (Figs 1–5).

DISCUSSION

We found that the conspicuity of some CVFs varied during different phases of the respiratory cycle and that in all cases, they were most conspicuous during inspiration. This finding suggests that for patients with SIH, myelography performed during maximum inspiration may aid in the detection of CVFs, thereby improving the overall diagnostic yield.

It is well-known that venous return is highly dependent on the respiratory phase.[9] Inspiration results in descent of the diaphragm causing negative intrathoracic pressure as well as increased intraabdominal pressure. This result creates a pressure gradient driving blood from the inferior vena cava to the right atrium, increasing venous return to the heart.[10] This blood flow also results in decreased intravascular pressure within the inferior vena cava, which would produce a gradient of pressure between the higher pressure CSF and the lower pressure epidural venous plexus and paraspinal veins.

In the setting of a CVF, we hypothesize that this gradient would result in rapid unregulated egress of CSF back into the circulatory system, with resultant increased conspicuity on myelography.[11] Conversely, during a Valsalva maneuver, the intrathoracic and inferior vena cava pressure considerably increases. This increase markedly reduces venous return and also eliminates the aforementioned pressure gradient between the CSF and the infradiaphragmatic venous system, which we hypothesize would reduce flow through a CVF.[12]

Our findings suggest that in cases in which a CVF is suspected, the diagnostic yield of spinal imaging may increase if it is performed during inspiration. In our practice, we now routinely perform our initial image acquisitions in this manner. This modification to the myelography technique is broadly applicable across modalities and can be used even in centers without the resources and equipment necessary to perform digital subtraction myelography.

This investigation is limited by the small number of cases reported and by its retrospective nature, which introduces the potential for selection bias. Furthermore, in our practice, some patients with CVF have not demonstrated changes in imaging conspicuity that are dependent on the phase of respiration. The proportion of patients with CVFs that are affected by differences in respiration remains unknown. Effort to answer this question as well as to determine the factors predictive of CVFs that exhibit imaging changes dependent on respiration is a logical direction for future research. Additionally, there may be other unknown factors related to respiration that result in changes to CVF conspicuity. For example, it is possible that there is a threshold at which substantially increased rates of venous return to the heart would result in rapid washout of contrast from a CVF, paradoxically reducing its conspicuity during inspiration.

CONCLUSIONS

The conspicuity of CVFs is improved during inspiration in some cases. Further investigation into the improved diagnostic performance of myelography performed during inspiration is warranted.

Disclosures: Linda Gray—*UNRELATED*: *Board Membership*: Spinal CSF Leak Foundation.

REFERENCES

1. Amrhein TJ, Kranz PG. **Spontaneous intracranial hypotension: imaging in diagnosis and treatment.** *Radiol Clin North Am* 2019;57:439–51 CrossRef Medline
2. Wang TY, Karikari IO, Amrhein TJ, et al. **Clinical outcomes following surgical ligation of cerebrospinal fluid-venous fistula in patients with spontaneous intracranial hypotension: a prospective case series.** *Oper Neurosurg (Hagerstown)* 2020;18:239–45 CrossRef Medline
3. Kranz PG, Gray L, Malinzak MD, et al. **Spontaneous intracranial hypotension: pathogenesis, diagnosis, and treatment.** *Neuroimaging Clin N Am* 2019;29:581–94 CrossRef Medline
4. Schievink WI, Maya MM, Jean-Pierre S, et al. **A classification system of spontaneous spinal CSF leaks.** *Neurology* 2016;87:673–79 CrossRef Medline
5. Kranz PG, Gray L, Amrhein TJ. **Decubitus CT myelography for detecting subtle CSF leaks in spontaneous intracranial hypotension.** *AJNR Am J Neuroradiol* 2019;40:754–56 CrossRef Medline
6. Headache Classification Committee of the International Headache Society (IHS). **The International Classification of Headache Disorders, 3rd Edition (Beta Version).** *Cephalalgia* 2013;33:629–808 CrossRef Medline
7. Dobrocky T, Grunder L, Breiding PS, et al. **Assessing spinal cerebrospinal fluid leaks in spontaneous intracranial hypotension with a scoring system based on brain magnetic resonance imaging findings.** *JAMA Neurol* 2019;76:580–87 CrossRef Medline
8. Kranz PG, Amrhein TJ, Gray L. **CSF venous fistulas in spontaneous intracranial hypotension: imaging characteristics on dynamic and CT myelography.** *AJR Am J Roentgenol* 2017;209:1360–66 CrossRef Medline
9. Pinsky MR. **Cardiopulmonary interactions: physiologic basis and clinical applications.** *Ann Am Thorac Soc* 2018;15:S45–48 CrossRef Medline
10. Willeput R, Rondeux C, De Troyer A. **Breathing affects venous return from legs in humans.** *J Appl Physiol Respir Environ Exerc Physiol* 1984;57:971–76 CrossRef Medline
11. Kumar N, Neidert NB, Diehn FE, et al. **A novel etiology for craniospinal hypovolemia: a case of inferior vena cava obstruction.** *J Neurosurg Spine* 2018;29:452–55 CrossRef Medline
12. Laborda A, Sierre S, Malve M, et al. **Influence of breathing movements and Valsalva maneuver on vena caval dynamics.** *World J Radiol* 2014;6:833–39 CrossRef Medline